SWASH ZONE CHARACTERISTICS AT OCEAN BEACH, SAN FRANCISCO, CA

L. H. Erikson[1], D.M. Hanes[2], P.M. Barnard[2], and A. E. Gibbs[2]

Runup data collected during the summer of 2005 at Ocean Beach, San Francisco, CA are analyzed and considered to be typical summer swash characteristics at this site. Analysis shows that the beach was dissipative with Iribarren numbers between 0.05 and 0.4 and that infragravity energy dominated. Foreshore slopes were mild between 0.01 and 0.05 with swash periods on the order of a minute. Predicted runup heights obtained with six previously developed analytical runup formulae were compared to measured extreme runup statistics. Formulations dependent on offshore wave height, foreshore slope and deep water wavelength gave reasonable results.

INTRODUCTION

The swash zone, defined as that part of the beach extending from a nearshore shallow depth to the limit of maximum inundation, is a relatively narrow region of great importance for the exchange of sediment between land and sea. Morphological processes such as storm-induced erosion, post-storm recovery, seasonal variation in foreshore shape, and evolution of rhythmic shoreline features are all driven by the inter-relationship between swash zone hydro- and sediment dynamics.

Much research has been done to understand and predict swash zone hydrodynamics and sediment transport (e.g., CSR 2006). Numerous experiments and datasets heave been collected from both the laboratory and field, and various numerical and analytical models have been developed with many significant improvements in recent years. It is now fairly well established that swash motion is driven by a combination of low frequency infra-gravity motions and incident wave bores which propagate up the beach face. The two mechanisms do not appear to be exclusive, but rather, one dominates over the other depending on the incident waves and foreshore slope.

One of the most important parameters in dealing with swash and morphological evolution is the runup length or height, defined as the limit of landward inundation. Figure 1 is a definition sketch showing a time-series of fluctuations of water elevation about its time-mean (set-up), and discrete water level elevation maxima, (R), referenced to the height above still water line (SWL). In this study, we present and analyze runup data measured during the

[1] G&G Environmental, 2601 Hambleton Lane, Santa Cruz, CA 95065 contracting to USGS

[2] Coastal and Marine Geology Program, U.S. Geological Survey, 400 Natural Bridges Drive, Santa Cruz, CA, 95060, USA

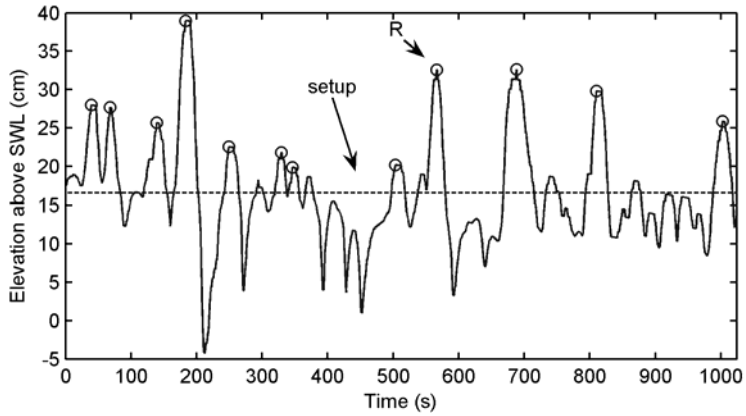

Figure 1. Definition sketch of a time-series showing swash oscillations, setup, and runup.

summer of 2005 at Ocean Beach, San Francisco, CA (Fig 2). Ocean Beach is a high-use recreation area located on the west side of San Francisco and within the Golden Gate National Recreation Area. The field effort in 2005 is part of an ongoing study that began in April 2004 to document, analyze, and simulate the processes that control sand transport and sedimentation patterns along Ocean Beach and the mouth of San Francisco Bay.

In the following sections, measurement methods and runup results are presented, followed by an assessment of the summer wave conditions and its affect on the runup limits. The paper then compares some previously developed analytical models to observed runup statistics.

Figure 2. Ocean Beach, San Francisco, CA study site (source: Google maps).

METHODS AND MEASUREMENT RESULTS

Time-series of runup elevations were determined by employing the method devised by Aagaard and Holm (1989) and Holland and Holman (1993 and 1999), whereby the leading edge of the swash is extracted from digital time-stacked images of a fixed cross-shore transect. A video camera, encased in a protective housing and mounted on top of the Cliff House Restaurant (http://www.evsboca.com/usgs/default.htm) at the north end of Ocean Beach, San Francisco, CA, collected four hours of video from which pixels along five predefined cross-shore transects (T1 through T5, approximately 50 meters apart) were extracted at 1 Hz (Fig. 3). A section of one of the time-stacks along transect 3 is shown in Fig. 3c. The location of the digitized leading edge was

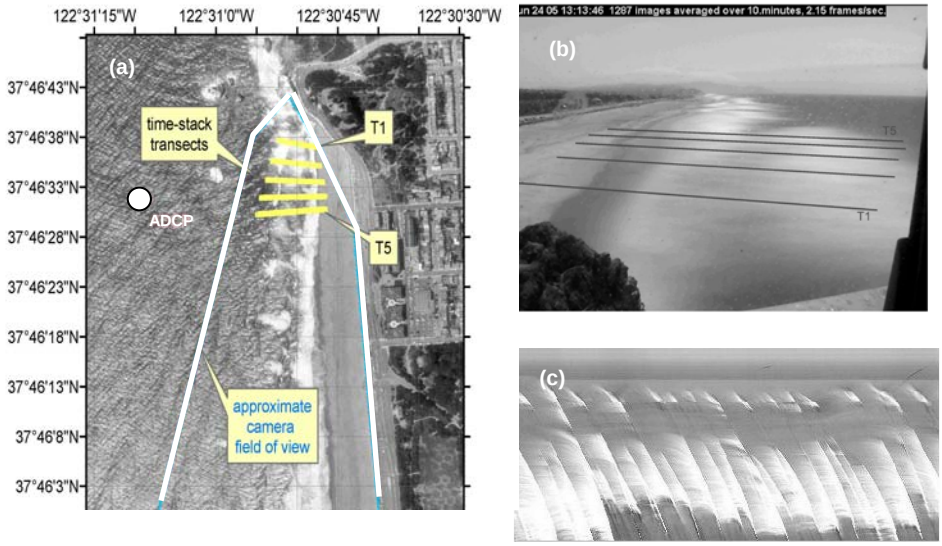

Figure 3. Overview of field measurements setup: (a) bird's-eye-view of camera, sampling transects, and location of offshore ADCP; (b) oblique camera view; (c) typical time stack image.

converted to real world coordinates with a transformation matrix determined from known ground control points, associated pixels, and assuming a plane beach (Holland et al. 1997). The resulting time-series from the time-stack images are leading edge swash motions obtained in a moving (LaGrangian) reference frame. The time-stack pixel resolution depends on the camera's position, field of view, and distance to target. For this particular setup it was 85 cm per pixel or better which, due to the mild beach slopes, translates to a vertical resolution of approximately 2 cm. Runup lengths were converted to runup heights, *R*, using a 'look-up table' of 1 meter-gridded beach topography measured with Differential Global Positioning Systems (DGPS) mounted on all terrain vehicles. Beach topography data at Ocean Beach were collected bi-

monthly by the USGS as part of the Coastal Evolution and Processes project; the dataset from June 27th 2005 was used for this study. It is recognized that runup height is dependent on beach slope, particularly for reflective beaches, and the use of beach topography data obtained three days *after* the runup data may introduce some error. However, due to the mild wave climate of the summer, the three day differential is not expected to affect the results greatly as exemplified with the topographical change measured 14 days prior to and 3 days following the runup experiment (mean absolute error MAE=0.30m, Fig. 4).

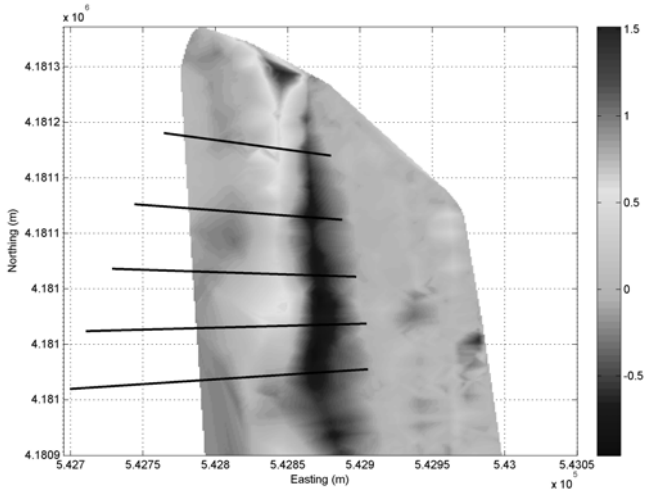

Figure 4. Beach topography change from June 12th to June 27th 2005. Black lines are cross-shore transect locations. Elevation in meters.

In order to minimize the effect of the rising tide on the location of wave breaking and area of active foreshore, and to provide consistency between the datasets, each four hour time-series at each transect was partitioned into ten 17-minute segments (1024 points at 1 Hz) for a total of $5 \times 10 = 50$ time-series. A best fit line through that part of the cross-shore profile corresponding to the minimum and maximum runup lengths during each 17-minute segment was used to define the active beach slope at each transect. Profiles of the five cross-shore transects are shown in Fig. 5. The beach slopes are mild ($\beta<0.1$) throughout but with an increase further up the coast at the two northern most transects T1 and T2 (max $\beta=0.05$).

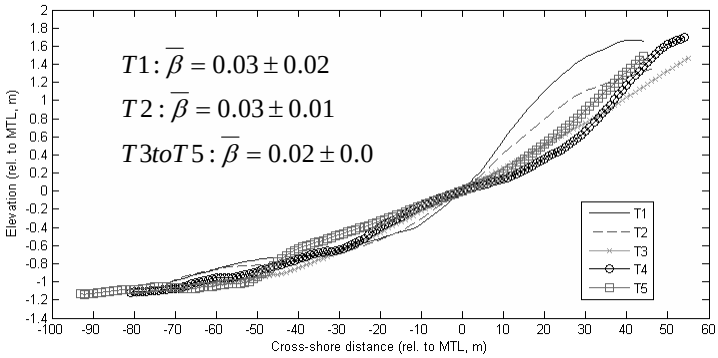

Figure 5. Cross-shore profiles along sampled time-stack transects.

Table 1. Measured and calculated offshore wave parameters.

	Measured		Back-calc deep water H_s (m)				Wave period (s)			
	H_s	h	H_o (T_{p1})	H_o (T_{p2})	H_o (T_{mo1})	H_o (T_{mo2})	T_{p1}	T_{p2}	T_{mo1}	T_{mo2}
min	1.01	7.69	0.90	1.02	1.08	1.10	13.29	9.31	6.71	6.10
max	1.35	8.49	1.18	1.31	1.46	1.47	13.47	10.20	7.42	6.81
stdev	0.12	0.29	0.10	0.10	0.13	0.13	0.06	0.30	0.26	0.25

Two runup statistics were focused upon in this study. The significant runup, R_s, was calculated as $R_s = 1.46 R_{rms}$ where R_{rms} is the root-mean-square runup height of discrete runup elevations determined from zero-down crossing in
the time-domain. The significant runup is statistically equivalent to the mean of the one-third highest runup elevations assuming a Rayleigh distribution. The second runup statistic is R_2, representing the runup height that is exceeded 2% of the time. The 2% runup was found by picking off the 98th percentile from the cumulative probability density function of the discrete runup measurements. Runup statistics listed in Table 2 were calculated following removal of the tide measured at the offshore ADCP (Fig. 3), are referenced to the still water level, and include setup and both infragravity and incident wave components. Distinctions between the infragravity and incident components are discussed later.

Wave parameters utilized in this study were measured with an RDI Workhorse Sentinel ADCP deployed outside the surf zone at 8m water depth (Fig. 3). Although the instrument collected data for over a week, it was quickly buried in the sand limiting further measurements, and hence, only data from the first day and coincident with the four-hour runup data is analyzed herein. Waves were measured at two hour intervals during 68 minutes of acoustic bursts at

2Hz. Bulk wave statistics were calculated from the resulting velocity spectra shown in

Table 2. Runup statistics and beach slope.

		T1		T2		T3		T4		T5	
	Local time (hh:mm)	R_s	R_2	R_s	R_2	R_s	R_2	R_s	R_2	R_s	R_2
1	**10:26**	14	21	13	17	13	19	17	23	25	36
2	**10:43**	17	27	18	26	14	23	18	30	24	34
3	**11:00**	13	19	24	35	21	24	38	48	21	36
4	**11:18**	23	34	25	36	20	23	31	44	20	27
5	**11:35**	33	46	33	46	23	31	22	29	24	31
6	**11:52**	28	43	30	42	25	45	18	20	18	27
7	**12:09**	32	49	22	34	21	32	16	19	21	32
8	**12:26**	34	46	36	56	20	26	13	20	18	26
9	**12:43**	45	56	39	57	23	34	16	26	22	31
10	**13:00**	40	50	42	51	21	29	19	28	25	39
	mean	28	39	28	40	20	29	21	29	22	32
	min	13	19	13	17	13	19	13	19	18	26
	max	45	56	42	57	25	45	38	48	25	39
	stdev	11	13	9	13	4	7	8	10	3	4

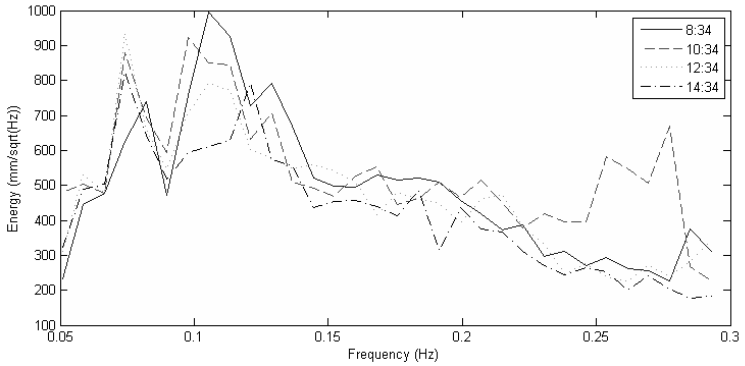

Figure 6. Velocity spectra measured with the ADCP (Site 1) concurrent with runup measurements on June 24th, 2005.

Fig. 6 with frequency cut-offs at 0.05 Hz and 0.30 Hz. The spectra show that the incident wave climate is bi-modal and hence two peak periods ($T_{p1} = 1/f_{p1}$ and $T_{p2} = 1/f_{p2}$, where f_p is the frequency at maximum energy) and mean periods ($T_{mo1} = m_0/m_1$ and $T_{mo2} = m_0/m_2$, where m_0, m_1, and m_2 are the zero'th, first, and second moments of the velocity PSD, and PSD is the power spectral

density) were calculated in addition to the significant wave height ($H_s = 4\sqrt{\sum(PSD)df}$). Bulk parameters were calculated for each of the four measured time-periods in Fig. 6 and linearly interpolated to time-windows of the runup data (Table 2). Because the instrument was positioned in transitional water, deep water significant wave heights were back-calculated employing the conservation of wave energy flux from linear wave theory via Eq. (1) and using the various measured wave periods:

$$H_o = H_h\left(\left(\frac{C}{2}\left(1+\frac{2kh}{\sinh(2kh)}\right)\right)\frac{4\pi}{gT}\right)^{0.5} \quad (1)$$

where H_h is the measured wave height at depth h, g is gravitational acceleration, C the phase speed (L/T), and k the wave number ($2\pi/L$). During the four-hour experiment, the significant wave height increased by about 35 cm while the incident wave period remained fairly constant at 13s, 10s, 7s, and 6s, for T_{p1}, T_{p2}, T_{mo1}, and T_{mo2}, respectively. The maximum peak energy switched over from a slightly shorter peak period, $T_{p2} \cong 10s$, to $T_{p1} \cong 13s$ about two-thirds of the way through the field study.

RUN-UP ANALYSES AND CHARACTERISTICS

Depending on beach slope and wave conditions, total runup is often described by two or three primary components (e.g., Komar 1998): (1) set-up of the mean water line due to radiation stresses induced by breaking waves (Longuet-Higgins and Stewart 1962); (2) fluctuations about that mean, due to the swash of incident waves producing runup and run-down (backwash); and (3) oscillations about the mean at infragravity frequencies, such that swash periods are greater than 20s, beyond the usual range of incident wave periods.

The runup time-series were band-pass filtered to determine the relative contributions of sea and swell (incident band, R_{inc}) $(0.05Hz < f < 0.2Hz)$ to infragravity (R_{ig}) $(f < 0.05Hz)$ components (Fig. 7). On average, the infragravity band contained 93% of the total runup variance, ranging from 84% (T1) to a maximum at T3 of 98%. The relative contribution of runup in the infragravity band to total runup (R_{ig}/R) was 0.83, similar to what Ruessink et al. (1998) found $(R_{ig}/R = 0.85)$, but less than the Oregon data set presented by Ruggiero et al. (2001 and 2004).

Runup energy density spectra were calculated using Welch's averaging method and a bandwidth of 9E-4 Hz for each of the 17-minute segments. Averages of the ten time-series segments are shown for each transect in Fig. 8. The dashed vertical line depicts the cutoff between infragravity and incident runup frequencies. It is clear that the peak energy lies within the infragravity

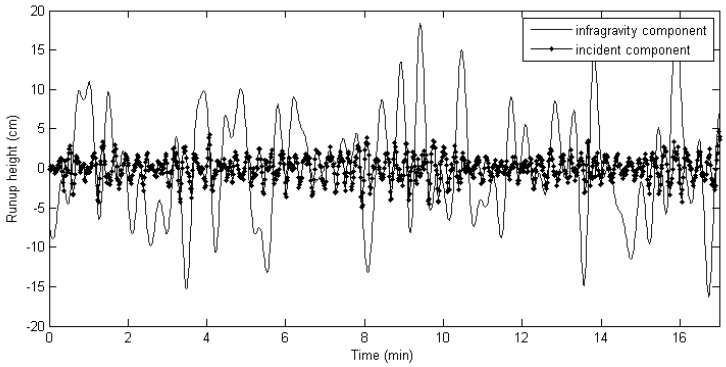

Figure 7. Typical 17-minute detrended time-series illustrating the dominant infragravity component (transect T3 on June 24, 2005, 10:09 to 10:23 am).

band and at incident band frequencies there is a steep drop-off in the energy. The peak periods ($1/f_p$) range from 41s to 68s with the longer periods (56s to 68s) observed at the three middle transects.

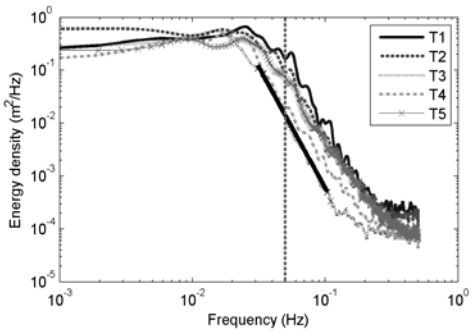

Figure 8. Total energy density (averaged over 10 subsequent 17-minute time-periods) measured at each cross-shore transect. Heavy solid line is best fit through T3 – rest are not shown. Dashed vertical line is cutoff between infragravity and sea swell frequencies.

The steep drop-offs in Fig. 8 suggest saturated surf and swash zones. Miche (1951) theorized that monochromatic incident waves consist of both a progressive and a standing wave component and that runup is proportional to the amount of shoreline reflection from the standing wave amplitude. The amplitude of the standing wave is depth limited as an increase in incident wave heights causes the breaking to occur further offshore, allowing energy dissipation through wave breaking, and less energy for swash. As such, saturation implies that the incident band runup height does not increase with increased offshore wave height.

Saturated runup energy density spectra have shown to decay as $E(f) = \alpha f^{-C}$, where α is a dimensionless constant (Huntley et al., 1977). Based on various field studies, the coefficient *c*, describing the degree of roll-off, is typically on the order of 3 to 4 (e.g., Guza and Thornton 1982; Ruessink et al.

1998; Raubenheimer and Guza 1996; Kobayashi et al. 1989; Ruggiero, et al. 2004). Best fit lines (Marquardt least-squares minimization) were fit through the roll-offs in Fig. 8 and found to range from c = 4.0 to as much as c = 4.8 at T3 (coefficients of determination were >0.95 for all five transects). At this time it is uncertain why the roll-off at T3 is larger than obtained at other sites.

Run-up dependencies

Although numerous factors influence the extent of swash oscillations (e.g., grain size, friction, turbulence, swash interaction, and infiltration to name a few), three parameters are generally considered to be strongly linked to observed runup statistics: offshore wave height (H_o), deepwater wave length (L_o=1.56T^2) and beach slope (β; $\tan(\beta) \cong \beta$ for mild slopes). Various combinations of these three parameters have been proposed, and in particular, there have been some recent developments in the prediction of runup on dissipative beaches. In this section, some of these dependencies and proposed analytical models are compared to the data obtained for this study.

In total, six different semi-empirically-based analytical models were used for the comparison: 1) Hunt, 1959; 2) Larson and Kraus 1989; 3) Mayer and Kriebel 1994; 4) Miche 1951, Guza et al. 1984, and Raubenheimer and Guza 1996; 5) Ruggiero et al. 2001, and 6) Stockdon et al. 2006. The last three were specifically developed with data from both reflective and dissipative beaches. Both Ruggiero et al. (2001) and Stockdon, et al. (2006) provide separate equations for strongly dissipative beaches, and although the data of this study shows that the site was dissipative under the measured summer conditions, there was an incident component that should not be ignored. In addition, employing equations that encompass both the incident and infragravity swash on dissipative beaches provides a broader spectrum of applicable scenarios.

Correlation coefficients (CODs) and root-mean-square-error (rmse) between measured and predicted runup elevations are summarized in Table 3. In order to assess the sensitivity of the models to the choice of bulk parameters obtained from the bimodal velocity spectra measured with the offshore ADCP, runup statistics were compared using the two peak periods (T_{p1} and T_{p2}) and mean representations (T_{mo1} and T_{mo2}). The choice of wave period affects both the wavelength and back-calculated deepwater wave height (H_o) whether reverse shoaling or conservation of energy flux is employed. In all cases, the significant runup height, R_s, is better correlated than the extreme runup statistic, R_2. This may be because the deepwater wave height used is the H_s, based on the same statistic as R_s ($R_s = 1.46R_{rms}$; $H_s = 1.46H_{rms}$). With respect to both the highest COD and smallest rmse, Hunt's original formula (1959) with either T_{mo1} or T_{mo2} appears to perform best overall (COD=0.70 and rmse=5cm, Fig. 9a). The relationship presented by Guza (1984) and others does not do as well even though it specifies a separate equation for saturated conditions which this dataset includes (see previous section). The relationship is independent of offshore wave height whereas all the others depend on H_o.

Table 3. Matrix of coefficients of determination (COD) and root-mean-square-error (rmse) between measured and predicted runup statistics.

COD/ Rmse	T_{p1}		T_{p2}		T_{mo1}		T_{mo2}	
	R_s	R_2	R_s	R_2	R_s	R_2	R_s	R_2
1)	0.71/18	0.66/10	0.72/9	0.67/8	*0.70/5*	0.66/13	0.70/5	0.65/15
3)	0.72/48	0.67/37	0.72/36	0.67/25	0.71/25	0.67/14	0.71/22	0.67/13
4)	0.71/22	0.66/13	0.69/12	0.64/9	0.63/6	0.61/13	0.62/6	0.60/14
5)	0.66/18	0.59/29	0.67/21	0.61/32	0.65/22	0.58/34	0.65/23	0.58/33
6)	0.71/45	0.67/35	0.70/30	0.65/19	0.70/17	0.66/9	0.70/14	0.66/7
7)	0.70/54	0.62/43	0.56/36	0.50/26	0.72/22	0.66/12	0.71/18	0.66/11

Because there was not much variation in the offshore wave height during the field experiment, a plot of runup versus H_o does not reveal any clear trend; rather, the dependency is inferred from the various runup models tested. The Mayer and Kriebel formulation does surprisingly well as it was not directly intended for dissipative conditions. However, their formulation addresses the physics behind the saturated surf and swash by incorporating the location of the break point and thus accounting for surf zone decay and consequently runup limited by depth-induced breaking. The location of the breakpoint, X_b, was estimated by assuming an equilibrium beach profile (A=0.11, based on D_{50}=0.30mm) and with a breaker index based on the non-dimensional Iribarren number, ε_o, (Iribarren and Nogales 1949; Battjes 1974; Kaminsky and Kraus 1993).

The formulations presented by Ruggiero et al. (2001) and Stockdon et al. (2006) perform about equally well except that the former appears to be somewhat less sensitive to the choice of wave period. Ruggiero et al.'s (2001) formulation was developed from both US west coast (Oregon) and East coast datasets, while Stockdon et al's is mostly from the East coast (but includes all of Ruggerio et al.'s data) with possibly less bimodal conditions. Ruggiero et al.'s formulation is quite similar to Hunt's original relationship except that Hunt has a stronger dependence on the beach slope (β vs $\sqrt{\beta}$). A least-squares fit to Ruggiero et al.'s governing parameter, $\sqrt{\beta H_o L}$, yields a coefficient of 0.27, equivalent to their empirical coefficient (Fig. 9b). It is expected that the empirical coefficient is dependent on some variables such as breaker type or friction. The median grain size at Ocean Beach is about D_{50}=0.27 mm (Barnard et al. under review), similar to the grain sizes of the datasets used by Ruggiero et al. (2001).

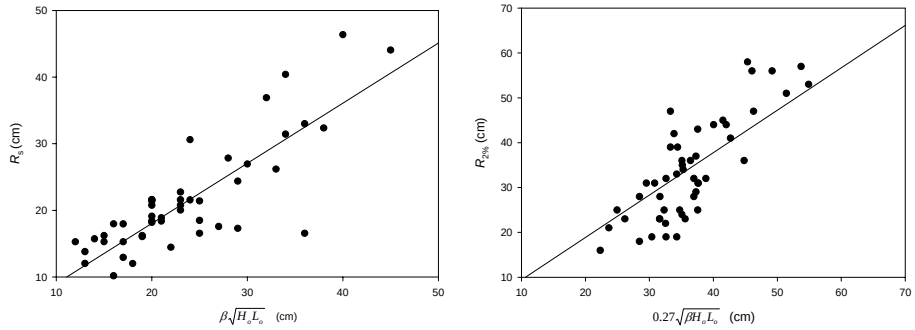

Figure 9. Measured runup statistics versus (a) Hunt's formula (1959), and (b) Ruggiero et al.'s (b) formulation. Both are shown with $T = T_{mo2}$.

SUMMARY AND CONCLUSIONS

Swash measurements were obtained along five cross-shore transects during a 4-hour sampling period on June 24th, 2005 at the north end of Ocean Beach, San Francisco. The data was band-partitioned into incident ($0.05Hz < f < 0.2Hz$) and infragravity ($f < 0.05Hz$) components and runup statistics were calculated separately and jointly. Beach slopes were mild ranging from 0.01 to 0.05, and analysis showed that the swash was dissipative with Iribarren numbers between 0.05 and 0.4 (using T_{mo2}). Infragravity components were dominant and made up approximately 80% of the total swash oscillation. Energy spectra of all measured runup data suggest that the surf and swash zones were saturated so that an increase in offshore wave height did not increase the runup as a significant portion of the incident waves were depth-limited breaking offshore. The spectra also indicate that the peak frequency of the swash ranged from 0.014Hz to 0.025Hz (i.e., swash periods between 40s and 70s).

An ADCP located just outside the surf zone of the cross-shore transects measured wave heights coincident with the runup data. Wave heights were on the order of 0.9m to 1.5m. Velocity spectra from the ADCP clearly show bi-modal conditions with incident peak wave periods ranging from 9s to 13.5s. Measured wave heights and periods were back-calculated to deep water conditions and used to predict the 2% and significant runup heights (R_2 and R_s, respectively). Predicted runup statistics using six previously published relationships were compared to field observations. It was found that Hunt's 1959 formula performed best when comparing to R_s, and Ruggiero et al.'s formulation (2001), which is similar to Hunt's but with less dependence on the foreshore worked well for predicting R_2. Using peak wave periods increased the root-mean-square-error (rmse) in all cases, while the mean period, in particular T_{mo2}, which is theoretically similar to the wave period obtained through zero-down crossing, gave results with the smallest rmse. In all, the analytical runup

formulations did quite well considering that Ocean Beach, and in particular the northern part of Ocean Beach, is strongly influenced by tidal currents (~1 m/s during the field study) and associated wave-current interactions. The relatively mild conditions of the summer may be partially responsible for this.

REFERENCES

Aagard, T. and D. Holm, 1989. Digitization of wave runup using video records, J. Coastal Res., 5, 547-551.

Barnard, P.L., J. Harney, and D. Rubin (under review). Field test comparison of an autocorrelation technique for determining grain size using a digital 'beachball' camera versus traditional methods**.** Sedimentary Geology, 21 pp.

Continental Shelf Research (CSR). 2006. Volume 26, Issue 5, Swash-Zone Processes, April 2006,

Battjes, J.A. 1974. Surf similarity, Proceedings of the 14th International Coastal Engineering conference, ASCE, Copenhagen, Denmark.

Guza,R.T. and E.B. Thornton. 1982. Swash oscillations on a natural beach. Journal of Geophysical Research, Vol. 87, pp. 438-491.

Holland, K.T. and R.T. Holman. 1999. Wavenumber frequency structure of infragravity swash motions, J. Geophys. Res. 104, 13,479-13,488.

Holland, K.T. and R.T. Holman. 1993. The statistical distribution of swash maxima on natural beaches, J. Geophys. Res. 87, 10,271-10,278.

Holland, K.T., R.T. Holman, and T. Lippman. 1997. Practical use of video imagery in nearshore oceanographic field studies. J. Oceanic Engr., 22(1), 81-92.

Holland, K.T., B. Raubenheimer, R.T. Guza, and R.A. Holman. 1995. Runup kinematics on a natural beach. J. Geoph. Res. 100 (C3), 4985-4993.

Holman, R.A. and R,T, Guza. 1984. Measuring runup on a natural beach. Coastal Engineering, 8, 129-140.

Holman, R.A. and A.H. Sallenger. 1985. Setup and swash on a natural beach. Journal of Geophysical Research, 90(C1), 945-953.

Hunt, I.A. 1959. Design of seawalls and breakwaters, J. Waterway Harbors Coastal Eng. ASCE, 85, 123-152.

Huntley D., R.T. Guza, and A.J. Bowen. 1977. A universal form for shoreline runup spectra? J. Geophys. Res. 82, 2577-2581.

Iribarren, R.R. and C. Nogales. 1949. Protection des Ports, proceedings from the XVIIth International Navigation Congress, Lisbon, Portugal.

Kaminsky, G.M. and N.C. Kraus. 1993. Evaluation of depth-limited wave breaking criteria, Proceedings of the Second International Symposium on Ocean Wave Measurements and Analysis. ASCE

Kobayashi, N., G.S. De Silva, and K.D., Watson. 1989. Wave transformation and swash oscillation on gentle and steep slopes, J. Geophys. Res., 94, 951-966.

Komar, P.D. 1998. Beach Processes and Sedimentation. Second Edition. Prentice-Hall, Inc.

Larson, M., and N.C. Kraus. 1989. "SBEACH: Numerical Model for Simulating Storm-Induced Beach Change. Report 1: Empirical Foundation and Model Development." Technical Report CERC-89-9. Coastal Engineering Research Center, U.S. Army Engineer Waterways Experiment Station, Vicksburg, MS.

Longuet-Higgins, M.S. and R.W. Stewart. 1962. Radiation stress and mass transport in gravity waves, with application to surfbeats, J. Fluid Mech., 13, 481-504.

Mayer, R.J. and D.L. Kriebel, 1994. Wave runup on composite-slope and concave beaches." 24th International Conference on Coastal Engineering, ASCE.

Miche, R. 1951. Le Pouvoir reflechissant des ouvrages maritimes exposes a l'action de la houle, Ann. Ponts Chaussees, 121,285-319.

Raubenheimer, B. and R.T. Guza. 1996. Observations and predictions of runup. J. Geophys. Res., 101, 25,575-25,587.

Ruessink, B.K., M.G. Kleinhans, and P.G.L. van den Beukel, 1998. Observations of swash under highly dissipative conditions, J. Geophysical Research, 103, 3111-3118.

Ruggiero, P., R.A. Holman, and R.A. Beach. 2004. Wave runup on a high energy dissipative beach, Journal of Geophysical Research, 109, 1-12.

Ruggiero, P., P.D. Komar, W.G. McDougal, J.J. Marra, and R.A. Beach, 2001. Wave runup, extreme water levels and the erosion of properties backing beaches, Journal of Coastal Research, 17(2), 407-419.

Stockdon, H.F., R.A. Holman, P.A. Howd, and A.H. Sallenger, Jr. 2006. Empirical parameterization of setup, swash and runup. Coastal Engineering, 53, 573-588.

ACKNOWLDEGEMENTS

The study was funded by the USGS Coastal Evolution Process-Based, Multi-Scale Modeling project. Many thanks are extended to Peter Ruggiero and Jodi Eshleman for insightful reviews and comments and Jodi Eshleman for rigorous wave data processing.